The EMBO Journal (2008) 27, 2363–2374 | © 2008 European Molecular Biology Organization | All Rights Reserved 0261-4189/08
www.embojournal.org

THE EMBO JOURNAL

The SpoMBe pathway drives membrane bending necessary for cytokinesis and spore formation in yeast meiosis

Peter Maier[1], Nicole Rathfelder[1], Celine I Maeder, Julien Colombelli, Ernst HK Stelzer and Michael Knop*

EMBL, Cell Biology and Biophysics Unit, Heidelberg, Germany

Precise control over organelle shapes is essential for cellular organization and morphogenesis. During yeast meiosis, prospore membranes (PSMs) constitute bell-shaped organelles that enwrap the postmeiotic nuclei leading to the cellularization of the mother cell's cytoplasm and to spore formation. Here, we analysed how the PSMs acquire their curved bell-shaped structure. We discovered that two antagonizing forces ensure PSM shaping and proper closure during cytokinesis. The Ssp1p-containing coat at the leading edge of the PSM generates a pushing force, which is counteracted by a novel pathway, the spore membrane-bending pathway (SpoMBe). Using genetics, we found that Sma2p and Spo1p, a phospholipase, as well as several GPI-anchored proteins belong to the SpoMBe pathway. They exert a force all along the membrane, responsible for membrane bending during PSM biogenesis and for PSM closure during cytokinesis. We showed that the SpoMBe pathway involves asymmetric distribution of Sma2p and does not involve a GPI-protein-containing matrix. Rather, repulsive forces generated by asymmetrically distributed and dynamically moving GPI-proteins are suggested as the membrane-bending principle.

The EMBO Journal (2008) **27,** 2363–2374. doi:10.1038/emboj.2008.168; Published online 28 August 2008
Subject Categories: membranes & transport; differentiation & death
Keywords: cell and organelle morphogenesis; GPI-anchored proteins; membrane shaping; phospholipase; sporulation

Introduction

It is a fundamental problem in cell biology to understand the mechanisms that lead to a specific shape of a membrane and how this relates to the function of an organelle. Membrane deformation and curvature can be influenced through the cytoskeleton, the shapes of peripheral or integral membrane proteins and through particular lipid compositions (McMahon and Gallop, 2005; Voeltz and Prinz, 2007). Previous investigations concentrated mainly on highly curved membranes, such as budding vesicles or tubulated organelles. However, much less is known about membrane curvature in the range of several hundred nanometers, which occurs, for example, during intracellular budding and different modes of autophagy.

Intracellular budding is a developmentally regulated way of cell division. Thereby, DNA segregation and the nuclear divisions (one, two or several rounds) are uncoupled from the physical cell separation process, leading to the formation of a syncytium. Each of the nuclei is then enwrapped by a *de novo* formed intracellular membrane system, which leads to cellularization within the boundaries of the original mother cell. This process is cytologically conserved in plants, pathogenic protists, fungi and yeasts (McCormick, 2004; Taxis and Knop, 2004). Examples include endosporulation during the host-specific vegetative life cycle of pathogenic ascomycetes like *Coccidioides immitis* (Miyaji *et al*, 1985) and during meiosis of model organisms such as *Saccharomyces cerevisiae* and *Schizosaccharomyces pombe* (Moreno-Borchart and Knop, 2003; Shimoda, 2004; Neiman, 2005).

In yeast meiosis, the new membrane systems are called prospore membranes (PSMs). PSM biogenesis starts at the onset of meiosis II with the homotypic fusion of secretory vesicles at the spindle pole bodies (SPBs), the centrosomes of yeast, which are embedded in the nuclear envelope (Moens and Rapport, 1971; Neiman, 1998; Knop and Strasser, 2000; Riedel *et al*, 2005). Initially, a PSM resembles a flattened pouch similar to a single Golgi cisterna. Constant vesicle fusion leads to the expansion of the PSMs. They acquire characteristic bell-like shapes while growing through the cytosol around the underlying nuclei. The forefront of the PSM is covered by the so-called leading edge protein coat (LEP coat, Figure 1A), which persists during PSM growth and consists of two coiled-coil proteins (Don1p and Ady3p) and Ssp1p, a protein essential for sporulation with functional resemblance to septins (Knop and Strasser, 2000; Moreno-Borchart *et al*, 2001; Maier *et al*, 2007).

During cytokinesis at the end of meiosis II, Ssp1p is removed from the LEP coat. This is sufficient to enable closure of the PSM forefronts (Maier *et al*, 2007) and leads to the formation of two stacked membrane bilayers surrounding the nuclei. The intervening space of these two membranes is then filled up with the different layers of the spore wall (Briza *et al*, 1986; Tachikawa *et al*, 2001). Whereas spore wall maturation is dependent on actin, PSM assembly and closure do not require the actin cytoskeleton (Taxis and Knop, 2006).

At present, it is unknown how the PSMs obtain their curved bell shape. Here, we identified constituents of the spore membrane bending (SpoMBe) pathway, which induces long-range membrane curvature along the PSM. We

*Corresponding author. EMBL, Cell Biology and Biophysics Unit, Meyerhofstrasse 1, 69117 Heidelberg, Germany. Tel.: +49 6221 3878631; Fax: +49 6221 3878631; E-mail: knop@embl.de
[1]These authors contributed equally to this work

Received: 23 January 2008; accepted: 31 July 2008; published online: 28 August 2008

characterized the respective contribution of this pathway as well as the LEP coat on PSM shape. Finally, detailed cell biological analyses of the SpoMBe propose a model, in which GPI-anchored proteins localize asymmetrically to the nucleus-proximal PSM bilayer and, owing to sterical repulsion, force the PSM to bend.

Results

Sma2p is required for PSM curvature in yeast meiosis

A systematic screen identified meiotically upregulated genes required for spore formation, called *SMA* genes (spore membrane assembly (Rabitsch *et al*, 2001)). The

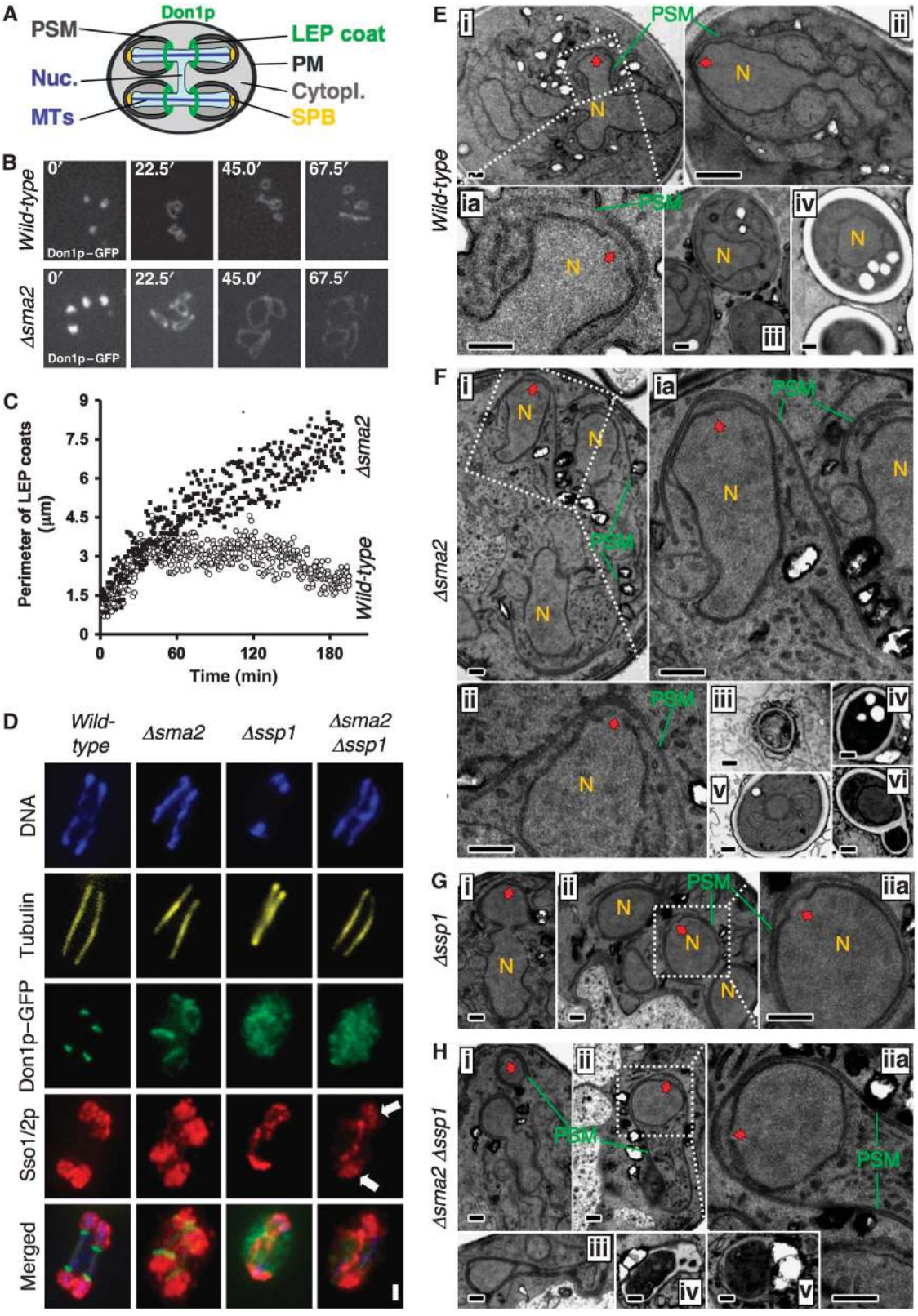

Δ*sma2* mutant progresses normally through the meiotic divisions (Rabitsch *et al*, 2001; Supplementary Figure S1), but it forms LEP coats with unusually large diameters and subsequently fails to form spores. We analysed the assembly and growth of the LEP coats in living cells with Don1p–GFP as a marker (Knop and Strasser, 2000) and quantified the LEP coat perimeters in wild-type and Δ*sma2* cells (Figure 1B and C, Supplementary Movies S1 and S2). During initial stages of LEP coat assembly, we could not identify any difference between the wild-type and the Δ*sma2* mutant. Once assembled, the size of the *wt*-LEP coat is limited to a circumference of ∼3 μm. However, in the Δ*sma2* mutant, it continuously grows during anaphase II up to more than 7 μm.

The increased LEP coats might be a secondary effect of their detachment from the PSM forefront or the consequence of oversized PSM openings. To distinguish these two possibilities, we used immunofluorescence microscopy and detected the LEP coats with anti-Don1p–GFP staining (Knop and Strasser, 2000) and the PSM surface with antibodies to the SNAREs Sso1p and Sso2p (Moreno-Borchart *et al*, 2001). In both wild-type and Δ*sma2* cells, the LEP coats are always associated with the PSMs, but in the Δ*sma2* mutant, the PSMs appear to be unusually broad (Figure 1D). In electron micrographs, the PSM openings of Δ*sma2* cells are much wider than in wild-type cells, and in large parts the PSMs grow straight (Figure 1E and F). The PSMs are only bended in the regions around the SPBs. In cells at later time points of sporulation, we sometimes observed unviable spore-like compartments (Figure 1F) that were unusually small and had the different layers of the spore wall aberrantly deposited.

Taken together, these observations indicate that Sma2p is not necessary for PSM biogenesis or growth *per se*, but it is required for PSM bending.

Sma2p-dependent PSM bending opposes the function of the LEP coat

Ssp1p is an essential component of the LEP coat. Without Ssp1p, the PSM forefronts close prematurely, which leads to tightly enwrapped nuclear fragments without enclosed cytoplasm (Figure 1G) (Moreno-Borchart *et al*, 2001; Maier *et al*, 2007). Therefore, the LEP coats might counteract a bending force that constantly pushes the PSM towards the nuclear envelope.

To test whether this curvature-generating force is independent of the LEP coat and dependent on Sma2p, we combined the Δ*sma2* with the Δ*ssp1* mutation. Immunofluorescence microscopy of the double mutant indicated that the PSMs occupy frequently a much wider area than the tubular structures observed in the Δ*ssp1* mutant (Figure 1D, white arrows). Using electron microscopy, we found that in the double mutant, the PSMs grew straight and significant amounts of cytoplasm, including some organelles, became enwrapped by the membranes (Figure 1H, ii and iii). Only in the region close to the SPB, the PSM sticks to the nuclear envelope (Figure 1H, i). In later stages of sporulation, spore-like bodies with deposited spore wall material were visible (Figure 1H, iv and v), similar to what was seen for the Δ*sma2* (Figure 1F) but never for Δ*ssp1* cells (Figure 1G).

Together, these findings suggest that deletion of both Δ*ssp1* and Δ*sma2* leads to a mixed phenotype, with structures reminiscent to the Δ*ssp1* mutant for regions close to the SPB, and otherwise with straight, non-curved PSMs. Therefore, Sma2p seems to facilitate PSM curvature independent of the LEP coat. Both Ssp1p and Sma2p constitute activities that exert opposing forces on the PSM.

SMA2 interacts genetically with SPO1, SPO19 and CWP1

We screened for genes that are able to suppress the Δ*sma2* sporulation phenotype when overexpressed by using haploid selection (Tong *et al*, 2001). In addition to the *SMA2* gene itself, *CWP1*, *SPO19* and an *ATG26* variant (deleted for the first 58 codons, termed Δ*N-ATG26*) suppressed the Δ*sma2* phenotype (Figure 2A). None of the identified genes suppressed the Δ*ssp1* mutation, demonstrating the specificity of suppression.

CWP1 and *SPO19* encode GPI-anchored proteins and suppress the sporulation defect of the Δ*spo1* mutation (Shimoi *et al*, 1995; Hamada *et al*, 1999; Tevzadze *et al*, 2000; Smits *et al*, 2006). Spo1p is homologous to a conserved protein family of phospholipases B and A2. Therefore, we tested the genetic relationship of *CWP1*, *SPO19*, *SMA2* and *SPO1*. *SPO19* and *CWP1* were also able to suppress the Δ*spo1* mutation in our assay, whereas *SMA2* was not able to suppress Δ*spo1*, nor was *SPO1* able to suppress Δ*sma2* (Figure 2A).

ATG26 is homologous to *PpATG26*, which is involved in autophagocytosis of peroxisomes (pexophagy) in the methylotropic yeast *Pichia pastoris*. It contains a C-terminally located UDP:glucose glucosyl transferase domain (Warnecke *et al*, 1999) and large N-terminal domains involved in targeting the protein to pexophagic structures (Oku *et al*, 2003).

Together, the genetic suppression analysis indicates that *SPO1* and *SMA2* are epistatic to each other, and that *CWP1*, *SPO19* and Δ*N-ATG26* are suppressors of both Δ*sma2* and Δ*spo1*.

Figure 1 Sma2p is required for PSM bending independent of the LEP coat. (**A**) Schematic drawing of a cell in anaphase of meiosis II. Cytopl., cytoplasm; Nuc., nucleus; PSM, prospore membrane; LEP coat, LEP coat of the PSM; SPB, spindle pole body; MT, meiosis II spindles; PM, plasma membrane. Don1p localizes to the LEP coat. (**B**) Live cell imaging of PSM growth in wild-type and Δ*sma2* cells using Don1p–GFP as a marker for the LEP coat. Supplementary Movies S1 (wild-type) and S2 (Δ*sma2*) are provided online. (**C**) Quantification of the LEP coat perimeters in the cells shown in (B). (**D**) Immunofluorescence localization of the markers Don1p–GFP (LEP coat) and Sso1/2p (PSM) in wild-type, Δ*sma2*, Δ*ssp1* and Δ*sma2* Δ*ssp1* cells. Cells were sporulated for 6 h where a high fraction of cells undergoes meiosis II, fixed and processed for immunofluorescence. Bar: 1 μm. (**E**) Electron micrographs of wild-type cells. N, nucleus; PSM, prospore membrane. (i) Overview and (ia) magnification of one entire PSM; (ii) PSM; (iii) immature and (iv) mature spore. (**F**) As for (E), but for Δ*sma2* cells. (i) Overview and (ia) magnification of one entire PSM; (ii) PSM; (iii–vi) spore-like bodies. (**G**) As for (E), but for Δ*ssp1* cells. (i and ii) Examples of PSMs, (iia) magnification of one PSM. (**H**) As for (E), but for Δ*ssp1* Δ*sma2* cells. (i–iii) Examples of PSMs, (iia) magnification of the nuclear associated area of a PSM; (iv and v) aberrant spore-like bodies. Bars: 300 nm. Strains and plasmids used in the figures are listed in Supplementary Table S1. (E–H) Red arrows point to spindle pole bodies (SPBs). For E–H, >30 cells with PSMs were investigated per strain. The shown situations are representative for each strain.

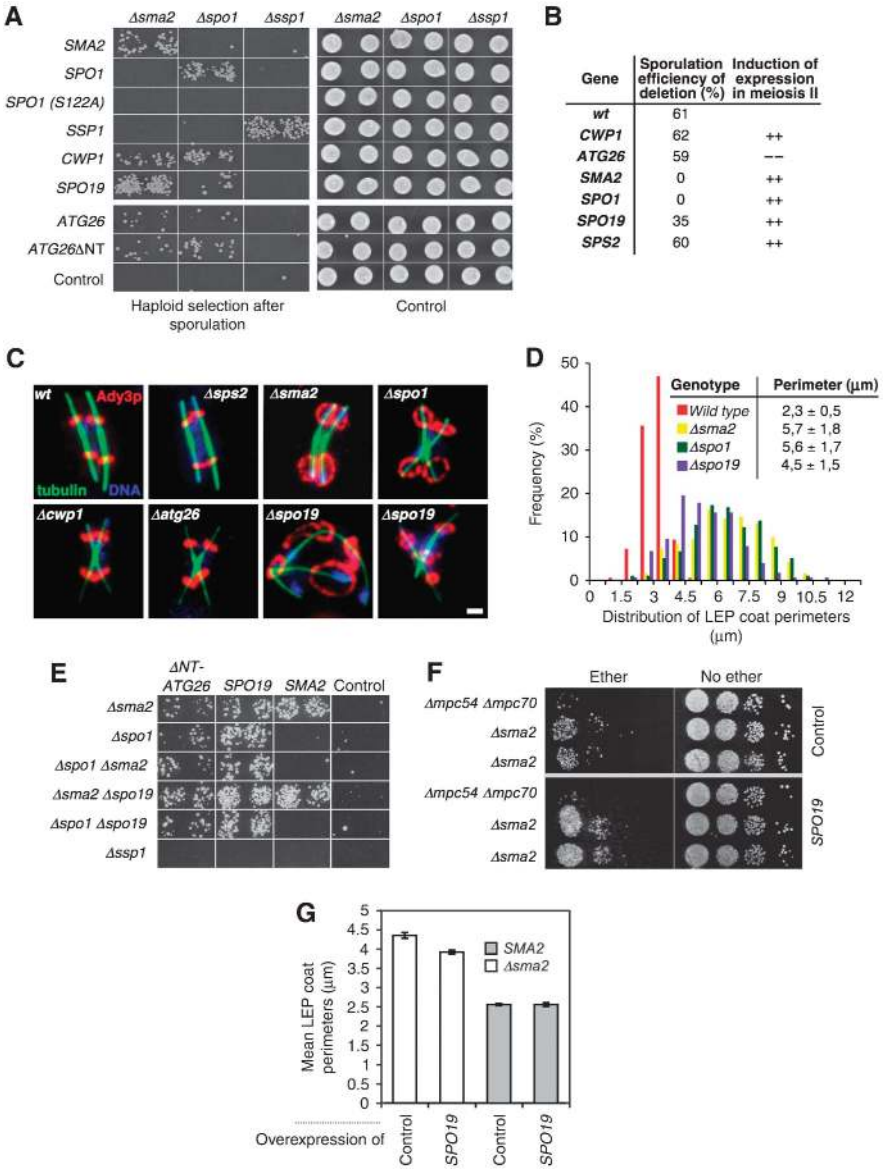

Figure 2 Characterization of high-copy suppressors of Δ*sma2*. (**A**) Deletion strains with a genetic background that allows selection for haploid cells (the products of meiosis and sporulation) (Tong *et al*, 2001) were transformed with high-copy (2 μm) plasmids harbouring the indicated genes. Equal amounts of liquid cultures were spotted on sporulation or control plates. Sporulated cells were replica-plated on haploid selection media and grown for 3 days. (**B**) Sporulation efficiency of deletion strains in the SK1 yeast strain background. The expression data during sporulation were taken from www.yeastgenome.org. (**C**) Immunofluorescence microscopy of wild-type and mutant cells (after 6 h of induction of sporulation) deleted for the indicated genes. Colour-merged pictures of typical cells in anaphase of meiosis II are shown. (**D**) Quantification of the LEP coat perimeters detected with the anti-Ady3p antibody in cells from the experiment shown in (C). Measurements were performed using maximum projections of image stacks across cells. (**E**) Suppression analysis by *SPO19* or Δ*N-ATG26* using single and double mutants (as indicated). (**F**) Suppression of Δ*sma2* by high-copy *SPO19* using resistance to ether vapour as an indication for the formation of spores (Rockmill *et al*, 1991) and SK1 yeast strains. (**G**) Perimeter of LEP coats measured in Δ*sma2* and wild-type cells expressing *SPO19* from a 2 μm plasmid. Error bars indicate the s.e.m. The difference between the LEP coat perimeters in the Δ*sma2* mutant with and without overexpressed *SPO19* is significant ($P<0.0001$). Measurements were done in intact cells (as compared to D). More experimental details are provided in Supplementary Figure S3A and the corresponding legend.

Spo1p and Spo19p function in the Sma2p-dependent PSM-bending pathway

To characterize the genes identified in the screen, we constructed deletion mutants, analysed their sporulation efficiencies (Figure 2B) and quantified the perimeters of the LEP coats (Figure 2C, quantification in 2D). Δ*cwp1* and Δ*atg26* mutants showed wild-type LEP coat sizes and sporulation efficiencies. However, the Δ*spo1* mutant did not sporulate, as reported previously (Tevzadze *et al*, 1996; Rabitsch *et al*, 2001) and the LEP coats were oversized, similar to the ones observed in the Δ*sma2* mutant. Similar to the Δ*sma2* mutant, also Δ*spo1* cells did progress normally through the meiotic divisions (Supplementary Figure S1). The Δ*spo19* mutant formed enlarged LEP coats, but the phenotype was less pronounced (Figure 2D). The Δ*spo19* mutant sporulated with a reduced sporulation efficiency of about 60% of the wild-type level (Figure 2B). This value dropped to about 40% when the Δ*spo19* mutation was combined with the Δ*cwp1* mutation (data not shown).

As the phenotypes of Δ*spo1*, Δ*sma2* and Δ*spo19* were similar, we constructed all possible double mutants and always observed oversized LEP coats (data not shown). We

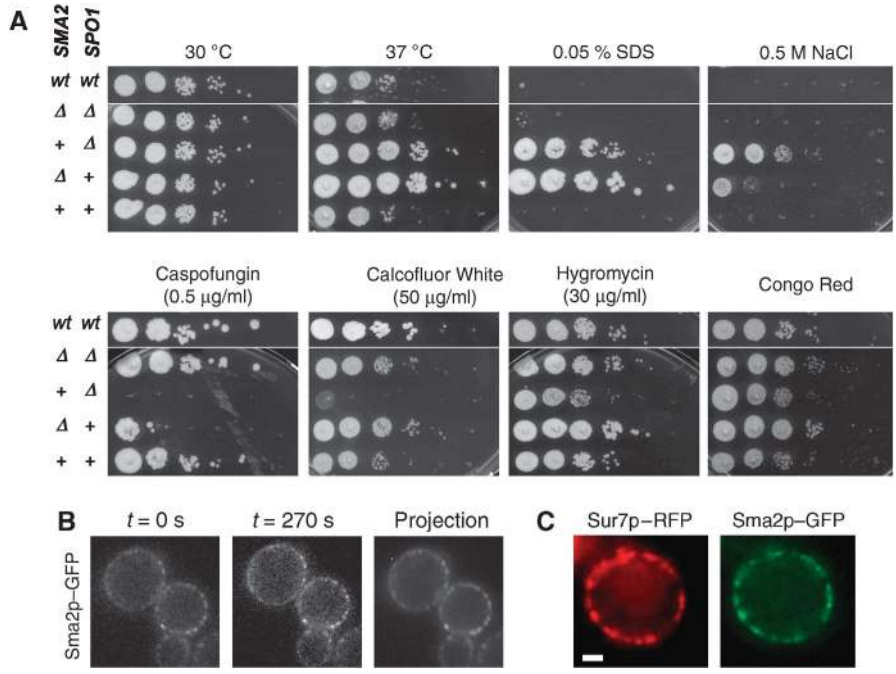

Figure 3 Expression of Spo1p and Sma2p leads to cell wall defects in vegetative cells. (**A**) Growth phenotypes of wild-type and mutant diploid cells. Genotypes as indicated; **Δ**, gene deletion; wt, wild-type; +, gene under control of the *CUP1* promoter (pr^{CUP1}). The *CUP1* promoter was induced with 50 μM $CuSO_4$ added to the growth media. (**B**) Vegetatively expressed Sma2p localizes to immobile cortical patches. Time lapse imaging of Sma2p–GFP expressing cells (from the *CUP1-1* promoter). Single planes across the middle of the cells (first and last frame of a time series) and the projection of the time series (300 frames taken during 270 s) are shown. (**C**) Colocalization of Sma2p–RFP and Sur7p–GFP to cortical patches in vegetative cells (quantification: Supplementary Figure S3B).

also tested whether these mutants are suppressed by high-copy Δ*N-ATG26* or *SPO19*. Both genes were able to suppress all double mutants including the Δ*sma2* Δ*spo1* mutant (Figure 2E).

These data indicate that *SMA2* and *SPO1* function in the same pathway required for PSM shaping. Furthermore, the partial defect of the Δ*spo19* mutant in the formation of correctly sized LEP coats correlates with a partial defect in spore formation and suggests that Spo19p is directly involved in PSM shaping.

Using ether resistance to test for spore formation, we found that high copy number expression of *SPO19* partially suppressed the Δ*sma2* mutation also in the SK1 yeast strain background (Figure 2F). We measured the perimeter of the LEP coats in Δ*sma2* cells that were arrested in late stages of meiosis II due to the Δ*ama1* deletion (Oelschlaegel *et al*, 2005) (Supplementary data and Supplementary Figure S2). This revealed weak but significantly decreased LEP coat perimeters as a function of *SPO19* overexpression (Figure 2G), consistent with the idea that the partial suppression is associated with a partial rescue of PSM bending.

Ectopic expression of Spo1p and Sma2p in vegetative cells interferes with cell wall function

We investigated the consequences of *SMA1* and *SPO1* expression in vegetative growing cells using the *CUP1-1* promotor (pr^{CUP1}). Both pr^{CUP1}-*SMA2* and pr^{CUP1}-*SPO1* strains often exhibited aberrant colony morphologies (data not shown). As this phenotype may be due to cell wall defects, we screened for synthetic effects when these strains were treated with conditions interfering with cell wall function (Figure 3A). *SPO1* or *SMA2* overexpression rendered the cells more sensitive to Caspofungin, which inhibits synthesis of β-1,3-glucan, a major cell wall component (Reinoso-Martin *et al*, 2003). Similarly, *SPO1* overexpression led to hypersensitivity against two chitin-remodelling inhibitors, Congo Red and Calcofluor White. In contrast, expression of either *SMA2* or *SPO1* increased cell viability at elevated temperatures, at high osmolarity (0.5 M NaCl) and in the presence of SDS, which perturbs membranes as well as the cell wall. We also observed that most of the phenotypes of single mutants could be reverted by overexpression of both genes simultaneously (Figure 3A). When we repeated most of these experiments using *GAL1*-promoter expression (instead of the *CUP1* promoter) and a different genetic yeast background (S288c), we obtained similar results (data not shown).

Sma2p–GFP localized to punctuate and static structures at the plasma membrane when ectopically expressed in vegetative cells (Figure 3B). Moreover, the Sma2p–GFP localization pattern significantly overlapped with that of Sur7p, a marker of specific cortical domains at the plasma membrane, the so-called Eisosomes (Figure 3C, Supplementary Figure S3) (Young *et al*, 2002; Malinska *et al*, 2004; Walther *et al*, 2006). A similar localization pattern was also found for Spo1p–9Myc (data not shown).

Together, these data indicate that *SMA2* and *SPO1*, when expressed alone, encode activities that disturb the formation of a fully functional cell wall. As several of these phenotypes are reverted upon overexpression of both genes, Sma2p and Spo1p appear to have individual functions that are neutralized (with respect to growth phenotypes) upon their coexpression in vegetative cells. This provides further evidence for a close functional relationship of both proteins.

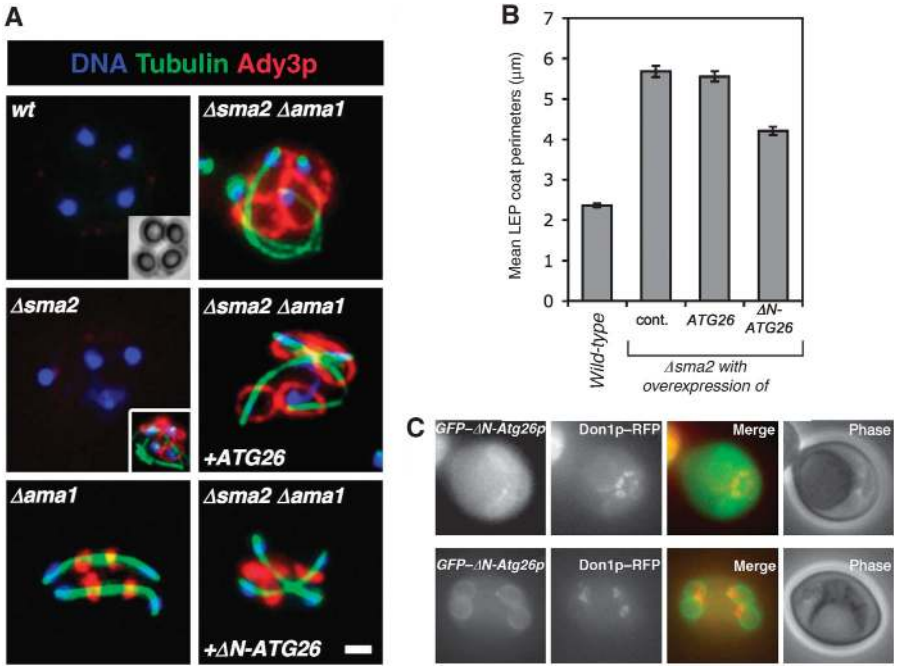

Figure 4 PSM-directed ΔN-Atg26p induces PSM curvature. (**A**) Immunofluorescence microscopy of cells 10 h after induction of sporulation. The *CUP1* promoter (pr^{CUP1}) was used to ectopically express ΔN-Atg26p and was induced with 7 μm $CuSO_4$ 4 h after induction of sporulation. The small inset in the wild-type picture shows the corresponding phase-contrast image. The inset in the Δ*sma2* panel shows a cell 6 h after induction of sporulation. (**B**) Quantification of the LEP coat perimeters in wild-type, Δ*sma2*, Δ*sma2* pr^{CUP1}–Δ*N-ATG26* and Δ*sma2* pr^{CUP1}–*ATG26* strains harbouring an additional Δ*ama1* deletion. Maximum projections of cells prepared as shown in (A) were used. Error bars indicate s.e.m. The difference between control cells and cells expressing Δ*N-ATG26* is significant ($P<0.00001$). (**C**) Localization of GFP–ΔN-Atg26p to PSMs in meiosis upon overexpression from the *CUP1* promoter. Don1p–RFP (using mCherry) labelling indicates the leading edge of the PSM.

PSM-localized ΔN-Atg26p induces ectopic PSM curvature

In contrast to *SPO1*, *CWP1*, *SPO19* and *SMA2*, *ATG26* is not meiotically upregulated (Figure 2B) and GFP tagging revealed that Atg26p is degraded during sporulation (Supplementary Figure S4). To investigate whether suppression of Δ*sma2* by N-terminally deleted (Δ*N*) *ATG26* occurs through re-bending of the PSM, we ectopically expressed Δ*N-ATG26* using chromosomal expression driven by the *CUP1-1* promoter, using the Δ*ama1* deletion background to synchronize the cells. Indeed, the LEP coat perimeters were considerably reduced in cells expressing Δ*N-ATG26* (Figure 4A, quantification is shown in Figure 4B). Consistent with a function of Atg26p in membrane bending, overexpressed GFP–ΔN-Atg26p localized to PSMs in addition to a cytoplasmic distribution (Figure 4C). Overexpression of full-length *ATG26* did only marginally decrease the size of the LEP coats. However, *ATG26* expressed from a high copy number plasmid suppressed Δ*sma2* weakly using the screen for haploid survival (Figure 2A). This might be due to the differences in strain background and the way *ATG26* was expressed (chromosomal expression using *CUP1-1* promoter versus high copy expression from a plasmid using the endogenous promoter).

In summary, rebending of the PSM seems to be sufficient to rescue the Δ*sma2* deletion. This supports the notion that the only essential function of Sma2p (and also Spo1p) for sporulation is the generation of PSM curvature.

Sma2p, Spo1p and Spo19p are meiosis-specific secretory proteins

Spo19p is predicted to be N-glycosylated and GPI-anchored similar to Cwp1p. In vegetatively growing cells, ectopically expressed Spo19p, as well as the endogenously expressed Cwp1p, are incorporated into the cell wall by covalent attachment to the β-glucan layer (Hamada *et al*, 1999), indicating that both proteins are secreted to the cell surface. Spo1p and Sma2p contain several motifs for N-glycosylation and one for translocation into the ER lumen. For Sma2p, three transmembrane domains and a large luminal domain at the N-terminus are predicted (Figure 5A). Spo1p is homologous to phospholipases A2 and B. The sequence is ~30% identical to Plb2p and encompasses a conserved putative lipid-binding pocket (^{89}SGGGYR^{94}) and the active site (^{120}G-x-S-x-G^{124}; Dessen *et al*, 1999). Unlike other phospholipases B, Spo1p has an insertion of ~70 aa directly C-terminal to its predicted catalytic site (Figure 5A). We mutated the assumed nucleophile (Ser^{122}) of the catalytic site to alanine and found that this mutant does not rescue the Δ*spo1* phenotype (Figure 2A).

Using tagged functional variants of Spo1p, Sma2p and Spo19p, we found that none of the proteins was expressed in vegetative cells growing on rich medium (Figure 5B and data not shown). Consistent with microarray data (Chu *et al*, 1998; Primig *et al*, 2000), Spo19p–GFP and Sma2p–3HA expression starts at the onset of meiosis II and PSM assembly (5 h after induction of sporulation). Spo1p–ProtA was already present in stationary phase cells grown on acetate containing media used for synchronous sporulation. The protein levels increased further during meiosis I and early meiosis II (starting at ~3.5 h in the meiotic time courses). We noticed an additional isoform of Spo1p–ProA in cells undergoing PSM assembly (5 to approx. 9 h), which was ~25 kDa smaller than the full-length protein (Figure 5B). The appearance of this smaller variant coincided with the expression of Sma2p–3HA and Spo19p–GFP, but its formation was not dependent on *SMA2* or *SPO19* (data not shown). Using tunicamycin treatment, we furthermore

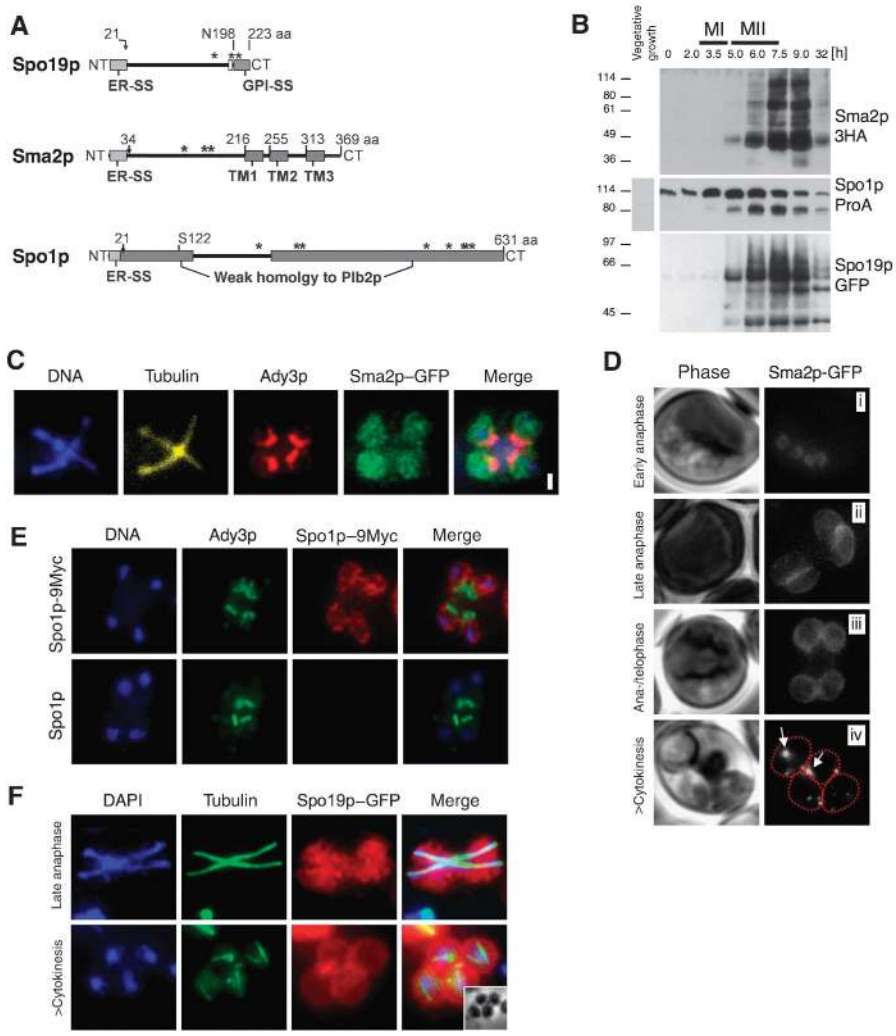

Figure 5 Spo19p, Sma2p and Spo1p are secreted components of the PSM. (**A**) Protein domain architecture of Spo19p, Sma2p and Spo1p. Abbreviations: ER-SS, signal sequence for translocation into the ER; TM, transmembrane domain; NT/CT, N-terminus/C-terminus. Asterisks (*) indicate potential *N*-glycosylation sites; GPI–SS, signal sequence for GPI-anchorage. (**B**) Western blot of Spo19p, Sma2p and Spo1p (using tagged constructs, as indicated) during sporulation time course experiments. Progression through sporulation was monitored using DAPI staining and found to be comparable in all three strains (not shown). MI and MII indicate the time points when most cells are in meiosis I or meiosis II. Position of molecular weight marker bands are as indicated. (**C**) Localization of Sma2p–GFP to the PSM using immunofluorescence microscopy. Sma2p–GFP, Ady3p, tubulin and DNA are detected as indicated. Bar, 1 μm. (**D**) Localization of Sma2p–GFP to the PSM (i–iii) and to the interior of mature spores (iv) using living cells. Representative cells are shown. (**E**) Localization of Spo1p–9Myc to the PSM using immunofluorescence microscopy. Spo1p–9Myc, Ady3p, tubulin and DNA are detected as indicated. A control cell expressing the untagged Spo1p is shown to indicate the specificity of the detection, as the expression level of Spo1p–9Myc was very low. (**F**) Localization of Spo19p–GFP to the PSM (top panel) and to the spore wall of immature spores (lower panel) using immunofluorescence microscopy.

found that Sma2p, Spo1p and Spo19p are glycosylated (Supplementary Figure S5). This confirms that these proteins traffic through the secretory pathway. Thereby we noticed that for Spo1p the lower molecular weight band was not formed anymore. This suggests that the smaller Spo1p isoform is a result of post-translational processing of Spo1p along the secretory pathway, as non-glycosylated proteins are likely to be retained in the endoplasmic reticulum. In solubilization assays, we confirmed that Sma2p is an integral membrane protein (data not shown). We also performed detergent phase-release experiments (on the basis of Triton-X114 fractionation and phospholipase C treatment (Bordier, 1981)) and found that in sporulating wild-type, Δ*sma2* and/or Δ*spo1* cells, Spo19p–GFP was always GPI-anchored (data not shown).

Taken together, Sma2p, Spo1p and Spo19p are secretory proteins specifically synthesized during meiosis and PSM formation. Moreover, Spo19p is a GPI-anchored protein and the presumed lipase activity of Spo1p is essential for its function during PSM shaping.

Sma2p, Spo1p, Spo19p and Cwp1p localize to the PSM

On the basis of immunofluorescence microscopy and live cell imaging data, Sma2p–GFP, Spo1p–9myc (Spo1p–GFP is not functional) and Spo19p–GFP localize to the entire PSMs in a uniform manner, similar to the syntaxins Sso1p and Sso2p (Figures 5C–F), consistent with the localization of Sma2p observed, when overexpressed (Nakanishi *et al*, 2007). Cwp1p–GFP can be detected on the PSM and at the plasma membrane of the cell (Supplementary Figure S6A) (Smits *et al*, 2006).

Previously, it has been shown that a putative GPI-specific phospholipase is essential for secretion of

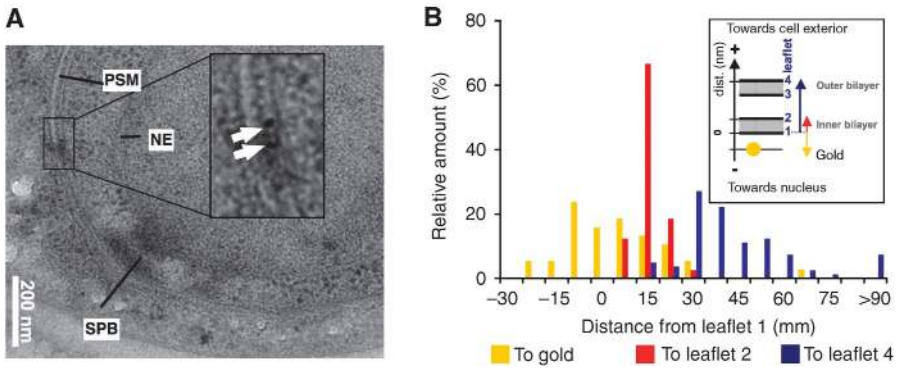

Figure 6 Sma2p localizes to the nucleus-proximal side of the PSM. (**A**) Immuno-electron microscopy of fixed yeast cells in meiosis II expressing Sma2p–GFP at endogenous levels. GFP was detected using specific antibodies and gold-labelled secondary antibodies. For more pictures, see Supplementary Figure S7. (**B**) Quantification of the position of gold for 35 cells. The distribution of the measured distances of the gold particles and the different membrane leaflets to leaflet 1 of the PSM is shown. The staining procedure does not directly visualize lipids, but rather proteins that are within the membrane and protrude to either side. Therefore, the innermost visible layer corresponds to the nucleus-proximal cytoplasmic side of the PSM. Usually, one or two gold grains were detected per PSM in the Sma2p–GFP strain, whereas no staining of PSMs was visible in control cells without GFP.

GPI-anchored proteins (Fujita *et al*, 2006) and that GPI-proteins might be necessary for the transport of specific membrane proteins (Okamoto *et al*, 2006). Moreover, secretion of Sma2p from the endoplasmic reticulum requires the Erv14p cargo receptor (Nakanishi *et al*, 2007). Therefore, we analysed whether Sma2p, Spo1p and Spo19p localization to the PSMs depends on each other. This was not the case (Supplementary Figure S6B and C and data not shown).

Sma2p localizes asymmetrically to the nucleus-proximal side of the PSM

In mature spores, Spo19p and Cwp1p were visible at the spore walls (Figure 5F and Supplementary Figure S6A and B). In contrast, Sma2p–GFP was only detectable as a punctuate signal in the interior of the spores (Figure 5D, arrows in iv). This may indicate that Sma2p–GFP is endocytosed, and thus, Sma2p—or at least a fraction of it—localizes specifically to the nucleus-proximal membrane of the PSM. Using immuno-electron microscopy of cells with open PSMs, we detected Sma2p–GFP only at the nucleus-proximal membrane of the PSM (Figure 6A, additional pictures are shown in Supplementary Figure S6). The observed distances of the gold grains to the two membranes of the PSMs indicated furthermore that the C-terminus of Sma2p (to which GFP is fused) is protruding into the cytoplasm (Figure 6B).

Rapid movement of GPI-anchored Spo19p within the PSM

When sporulating cells are treated with an inhibitor of GPI-anchor synthesis (Sutterlin *et al*, 1997), oversized LEP coats similar to the Δ*sma2* or Δ*spo1* mutants are formed (data not shown). To investigate the function of GPI-anchoring specifically for Spo19p and Cwp1p, we removed their putative GPI attachment sites and found that the corresponding mutants were no longer able to suppress the Δ*sma2* or Δ*spo1* phenotypes (Figure 7A). Interestingly, ΔGPI–Cwp1p–GFP still localized to the PSM (Figure 7B). This result suggests that the function of Cwp1p on the PSM and not the transport to the PSM requires GPI-anchoring.

The GPI-anchors of many proteins are cleaved at the plasma membrane of vegetative cells, and the proteins are attached to the β-glucan layer of the cell wall through their GPI remnant (Frieman and Cormack, 2004). Are Cwp1p and Spo19p also transferred to a (unknown) matrix present in the PSMs? We investigated this possibility in a photobleaching experiment of a Δ*spo19* strain complemented with a *SPO19–GFP*-containing plasmid. Repeated bleaching of a small region of the PSM led to rapid depletion of the entire GFP fluorescence from this particular PSM (Figure 7C, quantification in D), indicating rapid diffusion of Spo19p–GFP within the PSM. This result suggests that Spo19p is not covalently linked to any fixed matrix inside growing PSMs. Therefore, bending of the PSM is not achieved through a stable scaffold containing Spo19p. This is consistent with the notion that the different layers of the spore wall (harbouring also GPI-derived proteins) are synthesized not until the PSM closes during cytokinesis (Neiman, 2005). Moreover, *SPS2*, another meiotically upregulated GPI-anchored protein, which we found to suppress the Δ*sma2* and Δ*spo1* phenotypes (data not shown, Figure 2B and C), seems not to be attached to the cell wall when ectopically expressed in mitosis (Hamada *et al*, 1999).

Together, these data indicate that the suppressors of Δ*sma2* require GPI-anchoring for their function and suggest that GPI-anchored proteins are not incorporated into a cell wall matrix during PSM assembly.

Discussion

Spo1p, Sma2p and GPI-proteins comprise a luminal pathway necessary for PSM bending and regulated cytokinesis

Here, we report on the molecular players necessary for proper shaping of the PSMs and for cytokinesis during yeast meiosis and sporulation.

Genetic screening identified Spo1p, Sma2p and Spo19p as components of a novel and essential pathway underlying PSM bending. Several lines of evidence suggest that the only essential function of the SpoMBe pathway during meiosis and sporulation is to generate PSM curvature. SpoMBe mutants are unaffected in meiotic progression and the essential defect

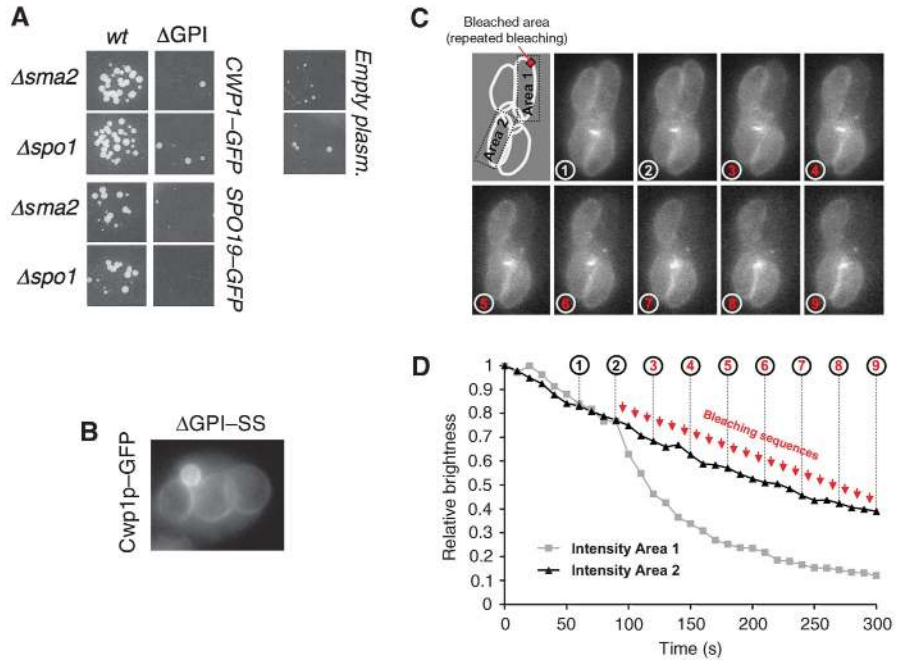

Figure 7 Rapid diffusion of Spo19p within the PSM. (**A**) The GPI-anchorage consensus sequence is required for Spo19p and Cwp1p to suppress the Δ*spo1* and Δ*sma2* mutants in sporulation. The assay was performed as described in Figure 2 using high copy number plasmids expressing the indicated alleles of *SPO19* and *CWP1*. Δ*GPI*: deletion of the GPI-anchorage consensus site, *wt*: wild-type. (**B**) The GPI-anchorage signal sequences of Cwp1p is not required for secretion of the protein to the spore wall. Live cell imaging of cells expressing Δ*GPI–CWP1–GFP*. Pictures of a representative cell were taken 10 h after induction of sporulation. (**C**) Diffusion of Spo19p within the PSM. For photobleaching, Spo19p–GFP was expressed from a low copy plasmid in a Δ*ama1* Δ*spo19* strain (Supplementary data). Time frames from one representative experiment ($n = 22$) with a cell in meiosis II are shown. (**D**) For quantification, the average brightness of the bleached (area 1) and one unbleached PSM (area 2) are shown. Repeated bleaching (time points indicated by red arrows) was conducted in a small area of one PSM, as indicated in (C). Stacks of five sections (spacing 0.83 μm) were recorded at 10 s intervals and maximum projections are shown.

can be rescued by ectopically induced PSM curvature due to overexpression of a truncated and mislocalized variant of *ATG26*, a gene normally involved in an autophagy-related process. Furthermore, the growth of the PSM *per se* is occurring normally in SpoMBe mutants. This suggests that the SpoMBe pathway functions specifically to generate PSM curvature.

The SpoMBe pathway is constituted of a luminal (Spo1p), a membrane protein with a luminal globular domain and a short cytoplasmic tail (Sma2p) and one major GPI-anchored protein (Spo19p). This argues that a luminal process of the PSM underlies membrane bending. Consistent with the notion that the curvature-generating force must be exerted in an asymmetric manner to achieve bending towards the side of the nucleus, Sma2p localizes exclusively to the nucleus-proximal membrane bilayer.

Epistasis experiments suggested that the membrane-bending force is exerted all along the PSM and that the LEP coat at the PSM forefront exerts an effect to counteract this force during PSM assembly. This ensures the incorporation of cytoplasmic content into the spore lumen and hinders the PSM from premature closure (Figure 8).

During cytokinesis, the LEP coat is disassembled in a regulated manner, and subsequently the PSMs close efficiently. This process is independent of an active contractile function at the PSM forefront, such as an acto-myosin ring (Moreno-Borchart *et al*, 2001; Taxis *et al*, 2006; Maier *et al*, 2007). Instead, the SpoMBe pathway seems to provide the necessary force that enables membrane closure (Figure 8C).

The direction of PSM curvature corresponds with asymmetrically distributed membrane proteins

Bending of the PSM and other organelles is intrinsically asymmetric and hence must depend on ways to apply forces onto the membrane in an asymmetrical manner, for example, through an asymmetric localization of the curvature-generating machinery. Indeed, Sma2p resides specifically to the nucleus-proximal bilayer of the PSM. Moreover, GPI-proteins cluster to the inner (nucleus-proximal) side of the spore wall, where they constitute the mannan layer of the spore wall (Neiman, 2005). Therefore, we hypothesize that during PSM growth, GPI-proteins also localize solely to the nucleus-proximal membrane. However, validation of this assumption is difficult due to the close proximity of the two membrane bilayers of the PSM (~40 nm), which prevents the precise localization of luminal proteins to one of the membranes by means of immuno-EM.

How is initial asymmetry of the PSM obtained and later maintained? Right after initiation of PSM assembly only the spindle pole body is known to touch the PSM on the nucleus-proximal side, and we hypothesize that this could be the origin of PSM asymmetry (Figure 8A).

During extension of PSMs, an unknown sorting mechanism seems to preserve asymmetry. Spo20p, a PSM-specific SNARE (Neiman, 1998) could function in this process, as in the Δ*spo20* mutant, PSM growth is reduced and LEP coats appear oversized, which points to defects in PSM curvature (Knop and Strasser, 2000; Neiman *et al*, 2000). Also, secretory vesicles accumulate near PSMs and this could indicate

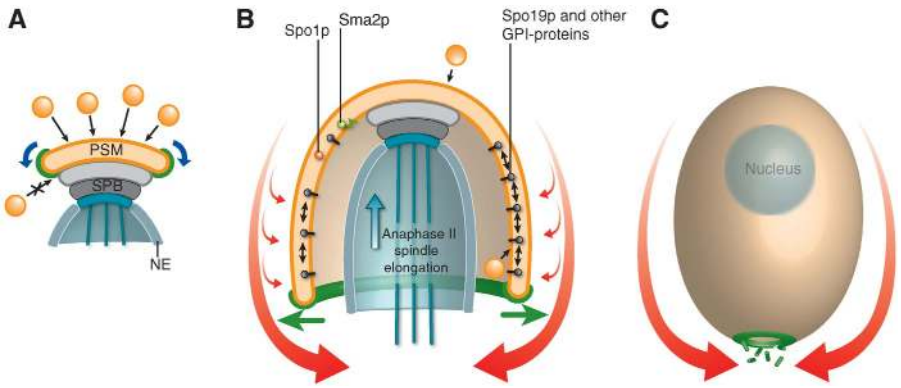

Figure 8 Model outlining the forces that possibly contribute to shaping and closure of the prospore membrane. (**A**) Upon initiation of the PSM at the SPBs by fusion of secretory vesicles, the LEP coat assembles at the forefront of the membrane. At this stage, delivery of vesicles can occur only at the SPB distal membrane, which might generate a membrane flux that directs the forefront of the membrane towards the side of the SPB/nuclear envelope (NE) (blue arrows). (**B**) Rapid movements of GPI-anchored proteins along the inner membrane (small red arrows) may generate repulsive forces that sums up to a force sufficient to drive long-range membrane bending of the PSM (red arrow). This force is selectively counteracted at the forefront of the membrane by the LEP coat (green arrows), which ensures a sufficient wide opening of the membrane necessary for cytoplasm and organelle inheritance. (**C**) During cytokinesis, selective closure of the PSM is achieved through the regulated removal of the LEP coat, in particular Ssp1p, from the forefront of the membrane.

asymmetry on the level of vesicle fusion with the PSM or a failure to deliver specific classes of exocytic vesicles containing cargo necessary for bending (SpoMBe components).

Spo1p and Sma2p seem to exert an effect on GPI-anchored proteins

In general, high-copy suppressors of null alleles can function through a parallel or unrelated pathway or downstream of the deleted gene in the same pathway. As deletion of *SMA2*, *SPO1* and their suppressor *SPO19* leads to almost identical phenotypes, *SPO19* seems to work in the same pathway, most likely downstream of *SMA2* and *SPO1*. This conclusion is further supported by the cell wall-related phenotypes observed during ectopic *SMA2* or *SPO1* expression in mitotic cells. In vegetative cells, these phenotypes could in principle be obtained by disturbance of many of the structures that compose the cell wall (mostly GPI-derived mannoproteins, glucan and chitin networks). However, the cell wall has only GPI-proteins in common with the PSM (Neiman, 2005). Assuming that the activities of Sma2p and Spo1p in mitosis and meiosis are identical could point to a mechanism where Sma2p and Spo1p exert an effect (directly or indirectly) on GPI-anchored proteins.

In vegetative cells, the associated phenotypes of ectopic expression of the single genes (*SPO1* or *SMA2*) is reverted by their simultaneous coexpression under most of the tested conditions. Moreover, high-copy *SPO1* does not suppress the Δ*sma2* mutation in meiosis and vice versa. Owing to this, Sma2p and Spo1p seem to function in close conjunction with each other, having either complementing or antagonizing activities.

What is the molecular function of Spo1p? The protein is homologous to the family of phospholipases A2 and B, which can hydrolyse or transacylate fatty acids from phospholipids and/or lysophospholipids (Fyrst *et al*, 1999; Merkel *et al*, 1999). A mutation in the putative active site inactivates Spo1p. However, no significant differences in the lipid patterns of PSM-enriched membrane fractions isolated from *wt* and Δ*sma2* and/or Δ*spo1* mutants were detected by lipid mass spectrometry (our unpublished data). With regard to our results, it is therefore tempting to speculate that Spo1p and maybe also Sma2p modify GPI-anchors. This requires an altered substrate specificity of Spo1p (in comparison with its homologues), which could be provided by the ~70 aa long insertion near the active site of Spo1p. It might be that they provide a mechanism to sort the GPI-anchored proteins such that their localization is also restricted to the nuclear-proximal membrane of the PSM. As a speculation, one could imagine a sorting mechanism where Spo1p excises GPI-anchored proteins from the peripheral membrane, whereas Sma2p causes their subsequent reinsertion into the nucleus-proximal membrane.

Previously, it was shown that a phospholipase A2 and an antagonizing enzyme exchange the fatty acids of GPI-anchored proteins. Moreover, the correct fatty acid content is essential for proper transport of GPI-proteins to their final destination and for segregation into specific membrane domains (Bosson *et al*, 2006; Fujita *et al*, 2006).

For Spo1p, a function of regulation of meiotic progression was suggested previously, and it was speculated that this was due to a function of lipid signalling. In our yeast strain background, we find no evidence for a function of Spo1p to promote meiotic progression (Supplementary Figure S1, Supplementary data).

A model of GPI-protein-dependent PSM shaping

Sma2p and Spo1p are present only at low—sometimes hardly detectable—amounts on the PSM. This makes it very unlikely that these proteins directly generate the physical force for PSM bending, for example, as a scaffold. They rather seem to function in an indirect way through Spo19p and other GPI-anchored proteins.

In meiosis II, almost 30 genes encoding GPI-anchored proteins are highly expressed (Chu *et al*, 1998; Primig *et al*, 2000). Most of these proteins are transported to the PSM, and upon cytokinesis, they are incorporated into the bulky mannan layer of the spore wall. Thereby, it seems that the GPI-anchors are cleaved and the proteins coupled to the glycan layer, which is assembled only after closure of the PSM (Tachikawa *et al*, 2001). Consistent with this, we found that Cwp1p and Spo19p are present in the detergent phase in Triton X-114 solubilization experiments in anaphase II cells (data not shown), indicating that they are GPI-anchored during PSM assembly. For Cwp1p and Spo19p, we further demonstrated that their suppressing activities depend on their

GPI-anchors. Therefore, GPI-anchoring on the PSM and not another (unknown, maybe enzymatic) feature of the proteins seems to enable suppression during PSM bending.

Assuming that GPI-proteins are asymmetrically targeted to the nucleus-proximal bilayer, their free diffusion within the membrane could induce PSM bending due to steric repulsion of their large and highly glycosylated protein heads attached to a comparatively small GPI-lipid (Figure 8B). This dynamic force would be needed during PSM assembly; consistent with this fact, we found that delayed expression of Sma2p after PSM formation fails to induce PSM bending (data not shown). Moreover, a dynamic bending mechanism would permit flexibility of the membrane. In fact, the PSM is often deformed in areas where it has to pave its way around an obstacle such as a mitochondrion that is imported in the developing lumen of the spore (Figure 1E).

Together, our results outline a new pathway how GPI-anchored proteins could shape organelles. These findings are of general interest, as the process of PSM shaping is cytologically conserved (e.g., in fungi) and also because the structure and function of the mammalian Golgi apparatus, for example, is dependent on GPI-anchored proteins (Li *et al*, 2007).

Materials and methods

Yeast strains and growth conditions

Yeast strains used in the experiments shown in Figures 1–7 are listed in Supplementary Table S1 and the genotypes are listed in Supplementary Table S2. Yeast chromosomal manipulations were done as described (Knop *et al*, 1999; Janke *et al*, 2004). Synchronous sporulation was performed as described previously (Alani *et al*, 1987). Sporulation medium contained 0.3% potassium acetate. Induction of protein expression from genes under control of the *CUP1* promoter (pr^{CUP1}) was done by addition of $CuSO_4$ to the liquid sporulation medium (7 μM) at the indicated time points. The final concentration of tunicamycin was 50 μg/ml. Growth phenotypes of vegetative strains overexpressing *SMA2* and/or *SPO1* under pr^{CUP1} control were assessed by spotting 5 μl of serial dilutions on YPD plates containing 100 μM $CuSO_4$ and 0.05% SDS, 2.5% K-acetate, 3% glycerol, 0.5 M NaCl, 0.5 μg/ml Caspofungin ('Cancidas', Merck & Co. Inc.), 50 μg/ml Calcofluor, 30 μg/ml Hygromycin or 150 μg/ml μM Congo Red. Sporulation efficiency and analysis of meiotic progression using DAPI staining was measured as described previously (Maier *et al*, 2007).

Genetic screen

Yeast strain YPM124 was transformed with a YEplac181-based library of yeast chromosomal fragments and grown on SC-Leu plates (~200 clones/plate, total of 37 000 clones). Cells were sporulated on plates and haploid cells were selected as described (Tong *et al*, 2001). For subcloning of *SMA2*, *SPS2*, *SPO19*, *SPO1* and *CWP1* genes, plasmid pRS426 was used and the subcloned genes were retested using strains YPM124, YNR80 and YNR82. pr^{CUP1} constructs of *ATG26* were made through insertion of a pr^{CUP1} containing cassette through PCR targeting (Janke *et al*, 2004).

Plasmid construction

Plasmids are listed in Supplementary Table S3. The bacterial strains used were DH5α and SURE. The *SPO1*, *SMA2*, *CWP1* and *SPS2* genes (ORF and ~350 bp upstream and downstream of the gene) were cloned using the 'gap repair' technique in ESM356-1. *SPO19* and *ATG26* were cloned using chromosomal DNA of strain ESM356-1 with primers designed to amplify ~350 bp of flanking sequences. The plasmids containing pr^{CUP1}–ΔNT-*ATG26* or pr^{CUP1}–*ATG26* were obtained in a similar way with the exception that chromosomal DNA of strains YPM183 or YPM208 was PCR-amplified and cloned. The *SPO19–GFP* construct was obtained by inserting a *NotI* site downstream of codon 26 using the quickchange method. Then, yeGFP (Knop *et al*, 1999) was cloned into the *NotI* site. Construction of mutant GPI-proteins: for mutants with impaired GPI-anchoring signal sequences (Δ*gpi–SS*), stop codons were introduced downstream of codon 217 (Cwp1p) or 196 (Spo19p).

Microscopic methods

For live cell imaging, a Leica DM RXA microscope, a Photometrics CoolSnap CF digital camera, fluorescent filter sets (Chroma) and Metamorph software were used. For image acquisition, sections throughout the cells (spacing of 0.4 μm) were collected using a *z*-axis focus drive and a ×100 Plan-Apo objective (aperture of 1.4; Leica). If not stated otherwise, maximum projections of the image stacks are shown. Movies of Don1p–GFP were obtained on an inverse PerkinElmer Ultraview LCI spinning disc confocal microscope, equipped with argon/krypton lasers (488 nm). Stacks of images were recorded every 90 s and maximum projections were obtained. Immunofluorescence microscopic procedures and antibodies were described before (Knop and Strasser, 2000; Riedel *et al*, 2005). LEP coat perimeters were measured using maximum projections of image stacks as mentioned above with the help of the 'trace region' command of Metamorph. The statistics on LEP coat measurements are shown in the Supplementary Table S3. Comparisons were based on *P*-values obtained using the Mann–Whitney *U*-test (http://elegans.swmed.edu/~leon/stats/utest.html).

$KMnO_4$ fixation electron microscopy was done as described (Neiman, 1998; Moreno-Borchart *et al*, 2001). Images were obtained on a Philips BioTwin CM120 electron microscope (100 kV accelerating voltage, TEM mode) equipped with a Keen View CCD camera (Soft Imaging System, Münster, Germany). Immuno-EM was performed as described (Muller-Reichert *et al*, 2003) (Supplementary data). Fluorescence loss in photobleaching was done on a wide field microscope using a laser scanner for photobleaching as described before (Taxis *et al*, 2005).

Supplementary data

Supplementary data are available at *The EMBO Journal* Online (http://www.embojournal.org).

Acknowledgements

We are grateful to Claude Antony, Ken Goldie, Charlotta Funaya, Anja Habermann and Uta Haselmann-Weiß for help with electron microscopy, and Timo Zimmermann and Stefan Terjung for help with microscopes. Charlie Boone, Jussi Jäntti, John Kilmartin and Frans Klis are kindly acknowledged for antibodies, plasmids and strains, Karl Kuchler for a gift of Caspofungin. We thank Björn Lohmann for dedicated assistance. The work was supported by a DFG grant (DFG KN498/2-2).

References

Alani E, Cao L, Kleckner N (1987) A method for gene disruption that allows repeated use of *URA3* selection in the construction of multiply disrupted yeast strains. *Genetics* **116:** 541–545

Bordier C (1981) Phase separation of integral membrane proteins in Triton X-114 solution. *J Biol Chem* **256:** 1604–1607

Bosson R, Jaquenoud M, Conzelmann A (2006) GUP1 of *Saccharomyces cerevisiae* encodes an *O*-acyltransferase involved in remodeling of the GPI anchor. *Mol Biol Cell* **17:** 2636–2645

Briza P, Winkler G, Kalchhauser H, Breitenbach M (1986) Dityrosine is a prominent component of the yeast ascospore wall. A proof of its structure. *J Biol Chem* **261:** 4288–4294

Chu S, DeRisi J, Eisen M, Mulholland J, Botstein D, Brown PO, Herskowitz I (1998) The transcriptional program of sporulation in budding yeast. *Science* **282:** 699–705

Dessen A, Tang J, Schmidt H, Stahl M, Clark JD, Seehra J, Somers WS (1999) Crystal structure of human cytosolic phospholipase A2 reveals a novel topology and catalytic mechanism. *Cell* **97:** 349–360

Frieman MB, Cormack BP (2004) Multiple sequence signals determine the distribution of glycosylphosphatidylinositol proteins between the plasma membrane and cell wall in *Saccharomyces cerevisiae*. *Microbiology* **150:** 3105–3114

Fujita M, Umemura M, Yoko-o T, Jigami Y (2006) PER1 is required for GPI-phospholipase A2 activity and involved in lipid remodeling of GPI-anchored proteins. *Mol Biol Cell* **17:** 5253–5264

Fyrst H, Oskouian B, Kuypers FA, Saba JD (1999) The PLB2 gene of *Saccharomyces cerevisiae* confers resistance to lysophosphatidylcholine and encodes a phospholipase B/lysophospholipase. *Biochemistry* **38:** 5864–5871

Hamada K, Terashima H, Arisawa M, Yabuki N, Kitada K (1999) Amino acid residues in the omega-minus region participate in cellular localization of yeast glycosylphosphatidylinositol-attached proteins. *J Bacteriol* **181:** 3886–3889

Janke C, Magiera MM, Rathfelder N, Taxis C, Reber S, Maekawa H, Moreno-Borchart A, Doenges G, Schwob E, Schiebel E, Knop M (2004) A versatile toolbox for PCR-based tagging of yeast genes: new fluorescent proteins, more markers and promoter substitution cassettes. *Yeast* **21:** 947–962

Knop M, Siegers K, Pereira G, Zachariae W, Winsor B, Nasmyth K, Schiebel E (1999) Epitope tagging of yeast genes using a PCR-based strategy: more tags and improved practical routines. *Yeast* **15:** 963–972

Knop M, Strasser K (2000) Role of the spindle pole body of yeast in mediating assembly of the prospore membrane during meiosis. *EMBO J* **19:** 3657–3667

Li X, Kaloyanova D, van Eijk M, Eerland R, van der Goot G, Oorschot V, Klumperman J, Lottspeich F, Starkuviene V, Wieland FT, Helms JB (2007) Involvement of a Golgi-resident GPI-anchored protein in maintenance of the Golgi structure. *Mol Biol Cell* **18:** 1261–1271

Maier P, Rathfelder N, Finkbeiner MG, Taxis C, Mazza M, Le Panse S, Haguenauer-Tsapis R, Knop M (2007) Cytokinesis in yeast meiosis depends on the regulated removal of Ssp1p from the prospore membrane. *EMBO J* **26:** 1843–1852

Malinska K, Malinsky J, Opekarova M, Tanner W (2004) Distribution of Can1p into stable domains reflects lateral protein segregation within the plasma membrane of living *S. cerevisiae* cells. *J Cell Sci* **117** (Part 25)**:** 6031–6041

McCormick S (2004) Control of male gametophyte development. *Plant Cell* **16** (Suppl)**:** S142–S153

McMahon HT, Gallop JL (2005) Membrane curvature and mechanisms of dynamic cell membrane remodelling. *Nature* **438:** 590–596

Merkel O, Fido M, Mayr JA, Pruger H, Raab F, Zandonella G, Kohlwein SD, Paltauf F (1999) Characterization and function *in vivo* of two novel phospholipases B/lysophospholipases from *Saccharomyces cerevisiae*. *J Biol Chem* **274:** 28121–28127

Miyaji M, Nishimura K, Ajello L (1985) Scanning electron microscope studies on the parasitic cycle of *Coccidioides immitis*. *Mycopathologia* **89:** 51–57

Moens PB, Rapport E (1971) Spindles, spindle plaques, and meiosis in the yeast *Saccharomyces cerevisiae* (Hansen). *J Cell Biol* **50:** 344–361

Moreno-Borchart AC, Knop M (2003) Prospore membrane formation: how budding yeast gets shaped in meiosis. *Microbiol Res* **158:** 83–90

Moreno-Borchart AC, Strasser K, Finkbeiner MG, Shevchenko A, Shevchenko A, Knop M (2001) Prospore membrane formation linked to the leading edge protein (LEP) coat assembly. *EMBO J* **20:** 6946–6957

Muller-Reichert T, Sassoon I, O'Toole E, Romao M, Ashford AJ, Hyman AA, Antony C (2003) Analysis of the distribution of the kinetochore protein Ndc10p in *Saccharomyces cerevisiae* using 3-D modeling of mitotic spindles. *Chromosoma* **111:** 417–428

Nakanishi H, Suda Y, Neiman AM (2007) Erv14 family cargo receptors are necessary for ER exit during sporulation in *Saccharomyces cerevisiae*. *J Cell Sci* **120:** 908–916

Neiman AM (1998) Prospore membrane formation defines a developmentally regulated branch of the secretory pathway in yeast. *J Cell Biol* **140:** 29–37

Neiman AM (2005) Ascospore formation in the yeast *Saccharomyces cerevisiae*. *Microbiol Mol Biol Rev* **69:** 565–584

Neiman AM, Katz L, Brennwald PJ (2000) Identification of domains required for developmentally regulated SNARE function in *Saccharomyces cerevisiae*. *Genetics* **155:** 1643–1655

Oelschlaegel T, Schwickart M, Matos J, Bogdanova A, Camasses A, Havlis J, Shevchenko A, Zachariae W (2005) The yeast APC/C subunit Mnd2 prevents premature sister chromatid separation triggered by the meiosis-specific APC/C-Ama1. *Cell* **120:** 773–788

Okamoto M, Yoko-o T, Umemura M, Nakayama K, Jigami Y (2006) Glycosylphosphatidylinositol-anchored proteins are required for the transport of detergent-resistant microdomain-associated membrane proteins Tat2p and Fur4p. *J Biol Chem* **281:** 4013–4023

Oku M, Warnecke D, Noda T, Muller F, Heinz E, Mukaiyama H, Kato N, Sakai Y (2003) Peroxisome degradation requires catalytically active sterol glucosyltransferase with a GRAM domain. *EMBO J* **22:** 3231–3241

Primig M, Williams RM, Winzeler EA, Tevzadze GG, Conway AR, Hwang SY, Davis RW, Esposito RE (2000) The core meiotic transcriptome in budding yeasts. *Nat Genet* **26:** 415–423

Rabitsch KP, Toth A, Galova M, Schleiffer A, Schaffner G, Aigner E, Rupp C, Penkner AM, Moreno-Borchart AC, Primig M, Esposito RE, Klein F, Knop M, Nasmyth K (2001) A screen for genes required for meiosis and spore formation based on whole-genome expression. *Curr Biol* **11:** 1001–1009

Reinoso-Martin C, Schuller C, Schuetzer-Muehlbauer M, Kuchler K (2003) The yeast protein kinase C cell integrity pathway mediates tolerance to the antifungal drug caspofungin through activation of Slt2p mitogen-activated protein kinase signaling. *Eukaryot Cell* **2:** 1200–1210

Riedel CG, Mazza M, Maier P, Korner R, Knop M (2005) Differential requirement for phospholipase D/Spo14 and its novel interactor Sma1 for regulation of exocytotic vesicle fusion in yeast meiosis. *J Biol Chem* **280:** 37846–37852

Rockmill B, Lambie EJ, Roeder GS (1991) Spore enrichment. *Method Enzymol* **194:** 146–149

Shimoda C (2004) Forespore membrane assembly in yeast: coordinating SPBs and membrane trafficking. *J Cell Sci* **117:** 389–396

Shimoi H, Iimura Y, Obata T (1995) Molecular cloning of CWP1: a gene encoding a *Saccharomyces cerevisiae* cell wall protein solubilized with *Rarobacter faecitabidus* protease I. *J Biochem (Tokyo)* **118:** 302–311

Smits GJ, Schenkman LR, Brul S, Pringle JR, Klis FM (2006) Role of cell cycle-regulated expression in the localized incorporation of cell wall proteins in yeast. *Mol Biol Cell* **17:** 3267–3280

Sutterlin C, Horvath A, Gerold P, Schwarz RT, Wang Y, Dreyfuss M, Riezman H (1997) Identification of a species-specific inhibitor of glycosylphosphatidylinositol synthesis. *EMBO J* **16:** 6374–6383

Tachikawa H, Bloecher A, Tatchell K, Neiman AM (2001) A Gip1p-Glc7p phosphatase complex regulates septin organization and spore wall formation. *J Cell Biol* **155:** 797–808

Taxis C, Keller P, Kavagiou Z, Jensen LJ, Colombelli J, Bork P, Stelzer EH, Knop M (2005) Spore number control and breeding in *Saccharomyces cerevisiae*: a key role for a self-organizing system. *J Cell Biol* **171:** 627–640

Taxis C, Knop M (2004) Regulation of exocytotic events by centrosome-analogous structures. *Topics Curr Gen* **10:** 193–207

Taxis C, Knop M (2006) System of centromeric, episomal, and integrative vectors based on drug resistance markers for *Saccharomyces cerevisiae*. *Biotechniques* **40:** 73–78

Taxis C, Maeder C, Reber S, Rathfelder N, Miura K, Greger K, Stelzer EH, Knop M (2006) Dynamic organization of the actin cytoskeleton during meiosis and spore formation in budding yeast. *Traffic* **7:** 1628–1642

Tevzadze GG, Mushegian AR, Esposito RE (1996) The SPO1 gene product required for meiosis in yeast has a high similarity to phospholipase B enzymes. *Gene* **177:** 253–255

Tevzadze GG, Swift H, Esposito RE (2000) Spo1, a phospholipase B homolog, is required for spindle pole body duplication during meiosis in *Saccharomyces cerevisiae*. *Chromosoma* **109:** 72–85

Tong AH, Evangelista M, Parsons AB, Xu H, Bader GD, Page N, Robinson M, Raghibizadeh S, Hogue CW, Bussey H, Andrews B, Tyers M, Boone C (2001) Systematic genetic analysis with ordered arrays of yeast deletion mutants. *Science* **294:** 2364–2368

Voeltz GK, Prinz WA (2007) Sheets, ribbons and tubules—how organelles get their shape. *Nat Rev Mol Cell Biol* **8:** 258–264

Walther TC, Brickner JH, Aguilar PS, Bernales S, Pantoja C, Walter P (2006) Eisosomes mark static sites of endocytosis. *Nature* **439:** 998–1003

Warnecke D, Erdmann R, Fahl A, Hube B, Muller F, Zank T, Zahringer U, Heinz E (1999) Cloning and functional expression of UGT genes encoding sterol glucosyltransferases from *Saccharomyces cerevisiae*, *Candida albicans*, *Pichia pastoris*, and *Dictyostelium discoideum*. *J Biol Chem* **274:** 13048–13059

Young ME, Karpova TS, Brugger B, Moschenross DM, Wang GK, Schneiter R, Wieland FT, Cooper JA (2002) The Sur7p family defines novel cortical domains in *Saccharomyces cerevisiae*, affects sphingolipid metabolism, and is involved in sporulation. *Mol Cell Biol* **22:** 927–934

